Supplement of Biogeosciences, 12, 3725–3740, 2015
http://www.biogeosciences.net/12/3725/2015/
doi:10.5194/bg-12-3725-2015-supplement

Biogeosciences Open Access

Supplement of

Patterns and persistence of hydrologic carbon and nutrient export from collapsing upland permafrost

B. W. Abbott et al.

Correspondence to: B. W. Abbott (benabbo@gmail.com)

Table S1. Upland thermokarst hydrologic flux extrapolated to the North Slope and circumarctic

	North Slope		Circumarctic	
	Mean	Range	Mean	Range
Extent of uplands/hills (10^6 km^2)*	0.24		1.83	
Percent of uplands susceptible to thermokarst**	37	(28-45)	37	(28-45)
Permafrost degrading by 2100 (%)***	93	(70-100)	68	(52-86)
Current upland thermokarst coverage (%)#	1.5	(1.2-1.8)	1.5	(1.2-1.8)
Upland thermokarst coverage by 2100 (%)	34	(20-45)	25	(15-39)
Current fluxes from thermokarst				
DOC (Tg C yr^{-1})	0.1	(0.04-0.2)	0.73	(0.30-1.4)
DIN (10^9 g N yr^{-1})	0.9	(0.04-0.2)	6.7	(2.8-14)
Projected fluxes from thermokarst (2050-2100)				
DOC (Tg C yr^{-1})	0.58	(0.16-1.2)	3.2	(0.92-7.5)
DIN (10^9 g N yr^{-1})	5.3	(1.5-12)	29	(8.5-78)

*Walker et al. 2005, **Zhang et al. 1999, ***Slater and Lawrence 2013, #Krieger 2012. See Appendix 1 for detailed treatment of assumptions. Projections of upland thermokarst dissolved organic carbon (DOC) and dissolved inorganic nitrogen (DIN) by the end of the century were calculated using: 1. The proportion of uplands susceptible to thermokarst as determined by ground ice content and landscape characteristics, 2. Daily yield for each development stage weighted by the duration of each stage and multiplied by growing season length, 3. Mean period of activity for each feature type, and 4. Regional and circumarctic projections of permafrost degradation. Estimates from the literature of period of activity (time spent in activity levels one and two) for slides, gullies, and slumps were 2, 8, and 20 years, respectively (Lewkowicz 1987, 1990, Burn 2000, Jorgenson and Osterkamp 2005, Lewkowicz 2007, Kokelj et al. 2009, Godin and Fortier 2012). However, because half of the slides in our study had triggered thaw slumps, substantially increasing their active lifespans, we estimated an 11-year period of activity for these features. We weighted period of activity for each feature morphology by the portion of current area for each morphology, yielding a mean active period of 11 years. Concerning future extent of permafrost, models project that 52-86% of circumarctic, near-surface permafrost will be degrading or isothermal by 2100, with estimates for the North Slope of Alaska ranging from 70-100%, based on representative concentration pathways RCP4.5 and RCP 8.5 (Slater and Lawrence 2013). However, nearly all of this change is expected to occur during the second half of the century for the continuous permafrost zone (Jafarov et al. 2013). Because we expected thermokarst activity to follow the same pattern, we calculated cumulative fluxes by 2100 divided by 50 to estimate annual thermokarst fluxes for 2050-2100. Given the compound assumptions associated with this extrapolation, we propagated error additively to obtain the range presented here.

References

Burn, C. R.: The thermal regime of a retrogressive thaw slump near Mayo, Yukon Territory, Can. J. Earth Sci., 37, 967–981, 2000.

Jafarov, E. E., S. S. Marchenko, and V. E. Romanovsky. 2012. Numerical modeling of permafrost dynamics in Alaska using a high spatial resolution dataset. Cryosphere **6**:613-624.

Kokelj, S. V., Lantz, T. C., Kanigan, J., Smith, S. L., and Coutts, R.: Origin and polycyclic be- haviour of Tundra Thaw Slumps, Mackenzie Delta Region, Northwest Territories, Canada, Permafrost Periglac., 20, 173–184, 2009.

Krieger, K. C.: The Topographic Form and Evolution of Thermal Erosion Features: a First Anal- ysis Using Airborne and Ground-Based LiDAR in Arctic Alaska, M.S. thesis, Geosciences, Idaho State University, Pocatello, Idaho, 98 pp., 2012.

Lewkowicz, A. G.: Nature and importance of thermokarst processes, Sand Hills Moraine, Banks Island, Canada Geogr. Ann. A, 69, 321–327, 1987.

Lewkowicz, A. G. 1990. Morphology, frequency and magnitude of active-layer detachment slides, Fosheim Peninsula, Ellesmere Island, N.W.T. Pages 111-118 *in* Permafrost-Canada: Proceedings of the Fifth Canadian Permafrost Conference. Centre d'études nordiques, Université Laval, Quebec City.

Lewkowicz, A. G.: Dynamics of active-layer detachment failures, Fosheim Peninsula, Ellesmere Island, Nunavut, Canada, Permafrost Periglac., 18, 89–103, 2007.

Slater, A. G. and Lawrence, D. M.: Diagnosing present and future permafrost from climate models, J. Climate, 26, 5608–5623, 2013.

Walker, D. A., Raynolds, M. K., Daniels, F. J. A., Einarsson, E., Elvebakk, A., Gould, W. A., Katenin, A. E., Kholod, S. S., Markon, C. J., Melnikov, E. S., Moskalenko, N. G., Talbot, S. S., Yurtsev, B. A., and Team, C.: The Circumpolar Arctic vegetation map, J. Veg. Sci., 16, 267– 282, 2005.

Zhang, T., Heginbottom, J. A., Barry, R. G., and Brown, J.: Further statistics on the distribution of permafrost and ground ice in the Northern Hemisphere, Polar Geography, 24, 126–131, 2000.

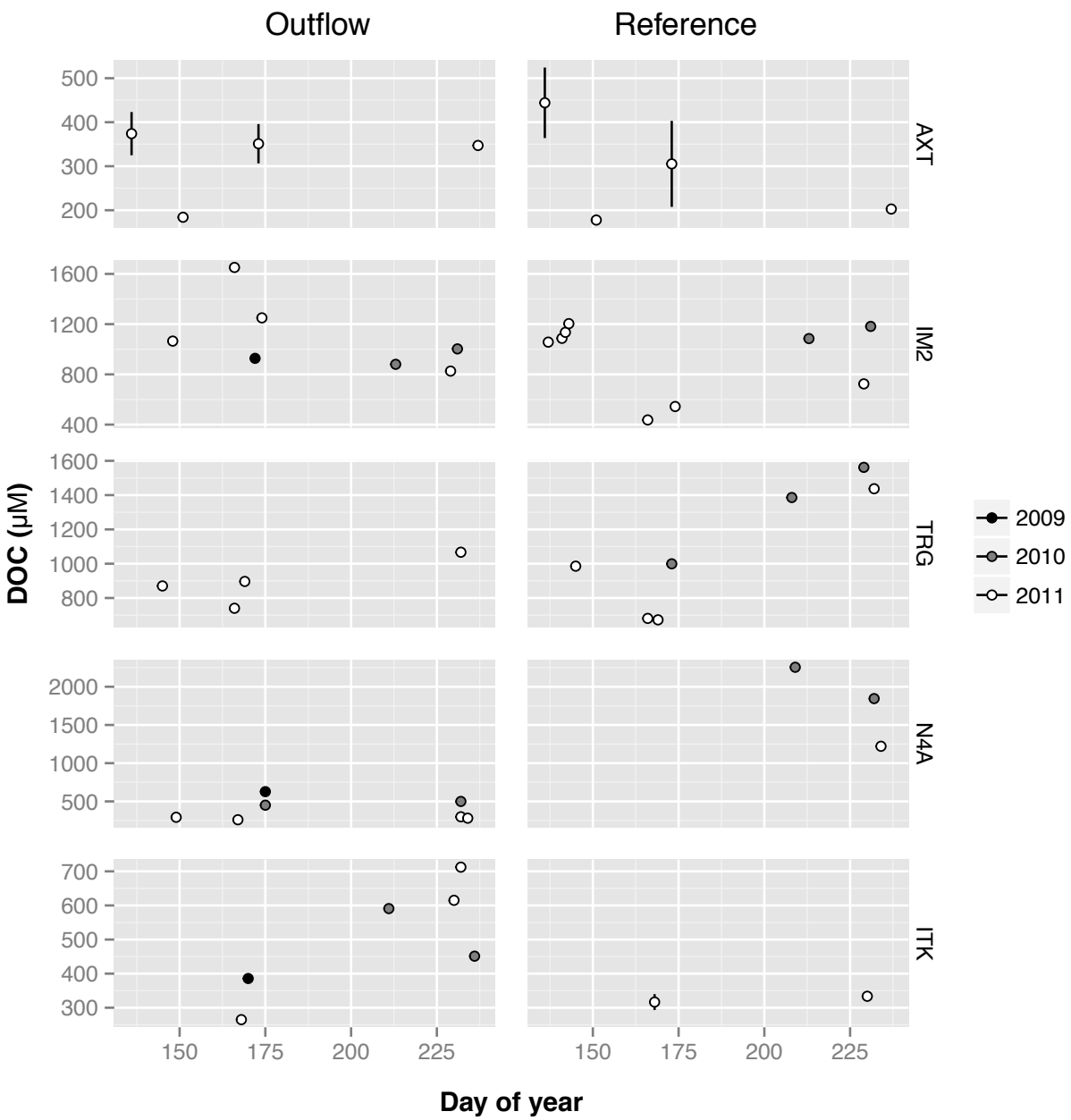

Figure S1. Dissolved organic carbon (DOC) concentration for water draining thermokarst features (outflow) and paired unimpacted water body (Reference) for the five sites near the Toolik Field Station where repeat measurements of feature outflow were made from 2009-2011. Site AXT was an active layer detachment slide, sites IM2 and TRG were thermo-erosion gullies, and sites N4A and ITK were retrogressive thaw slumps. Error bars represent standard error for sites where more than one outflow or reference water was sampled on the same date.

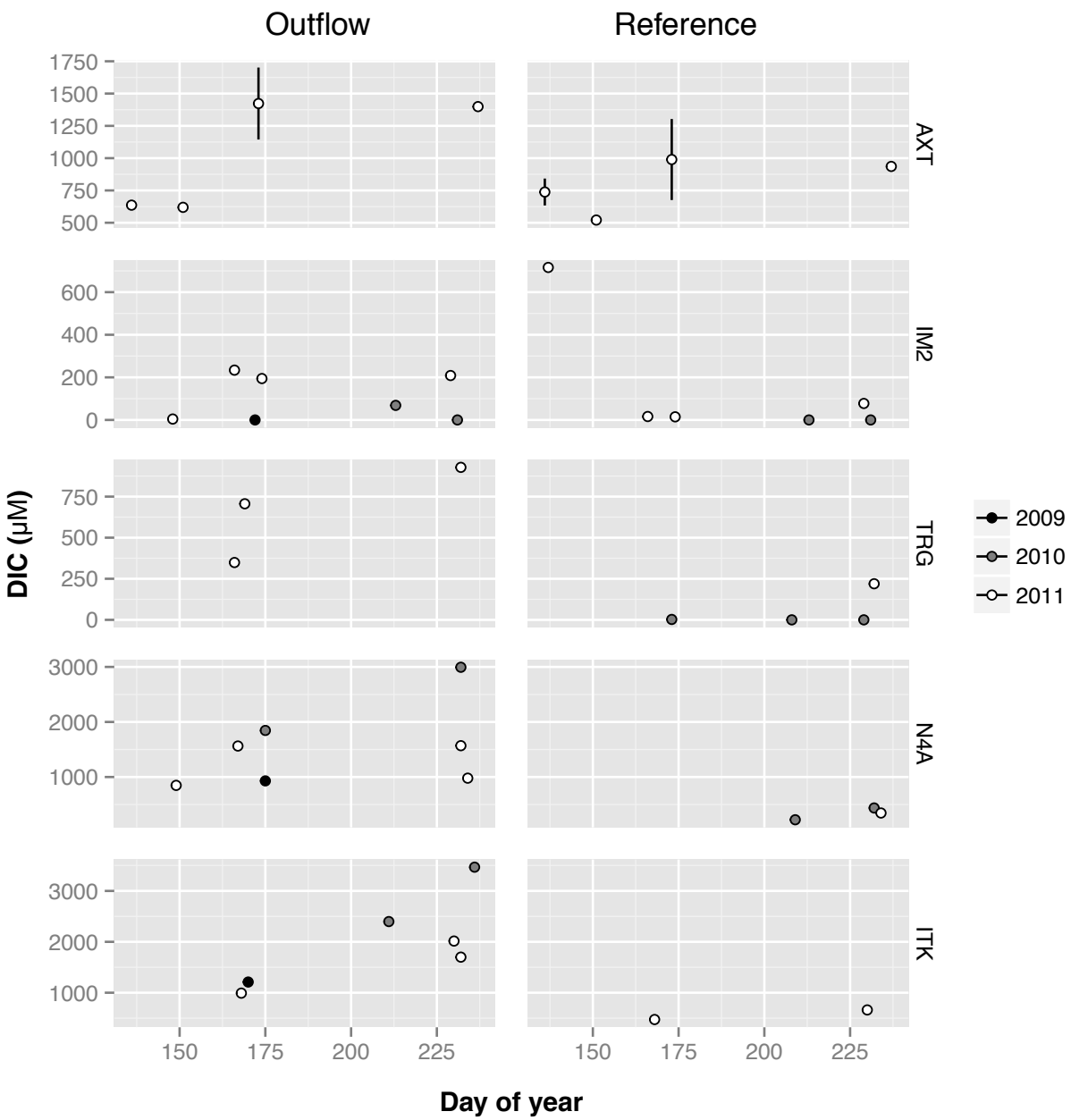

Figure S2. Dissolved inorganic carbon (DIC) concentration for the five sites near the Toolik Field Station where repeat measurements of feature outflow were made from 2009-2011. Symbology as in figure S1.

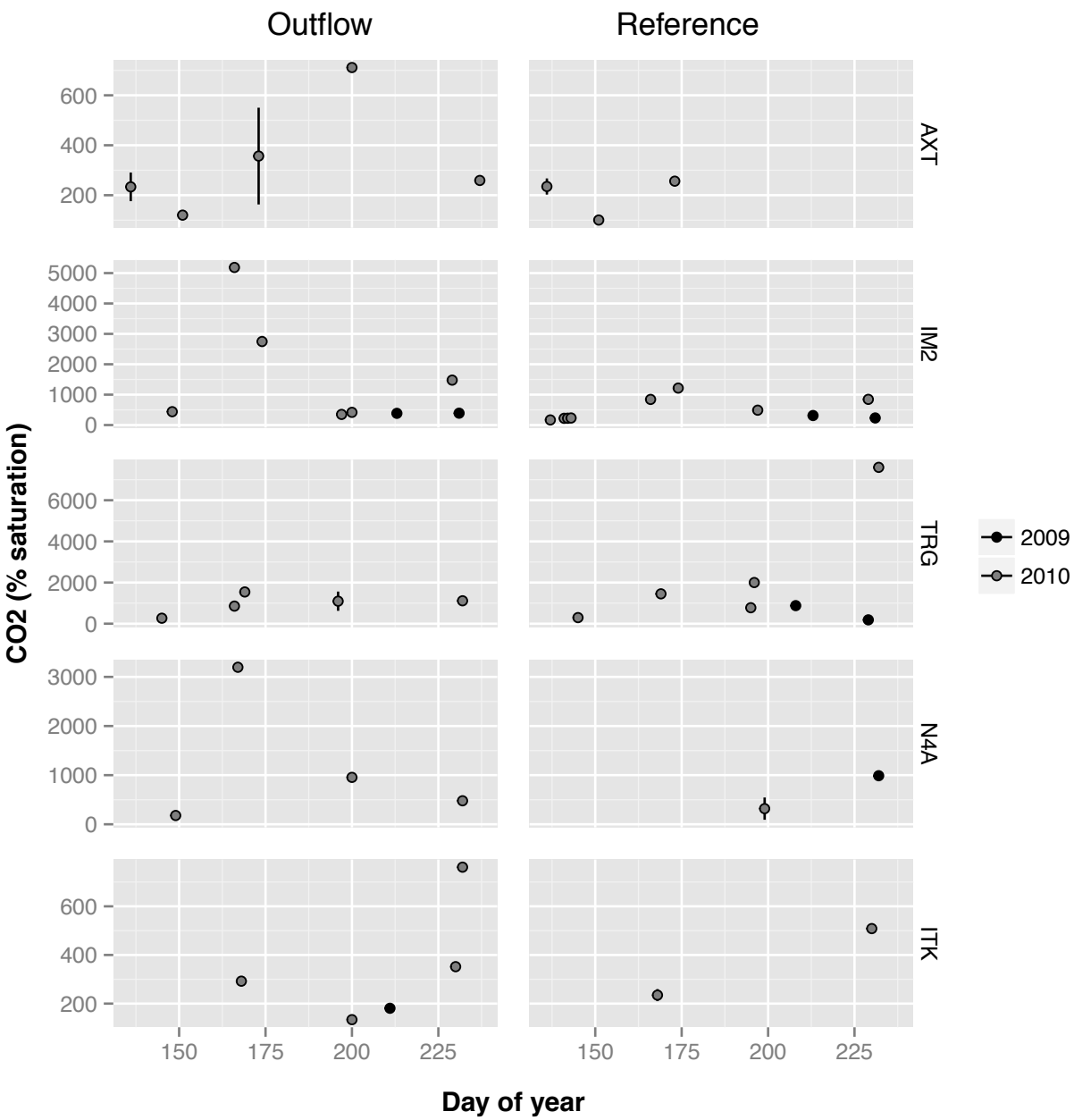

Figure S3. Dissolved CO_2 in % equilibrium concentration based on water temperature for the five sites near the Toolik Field Station where repeat measurements of feature outflow were made from 2009-2011. Symbology as in figure S1.

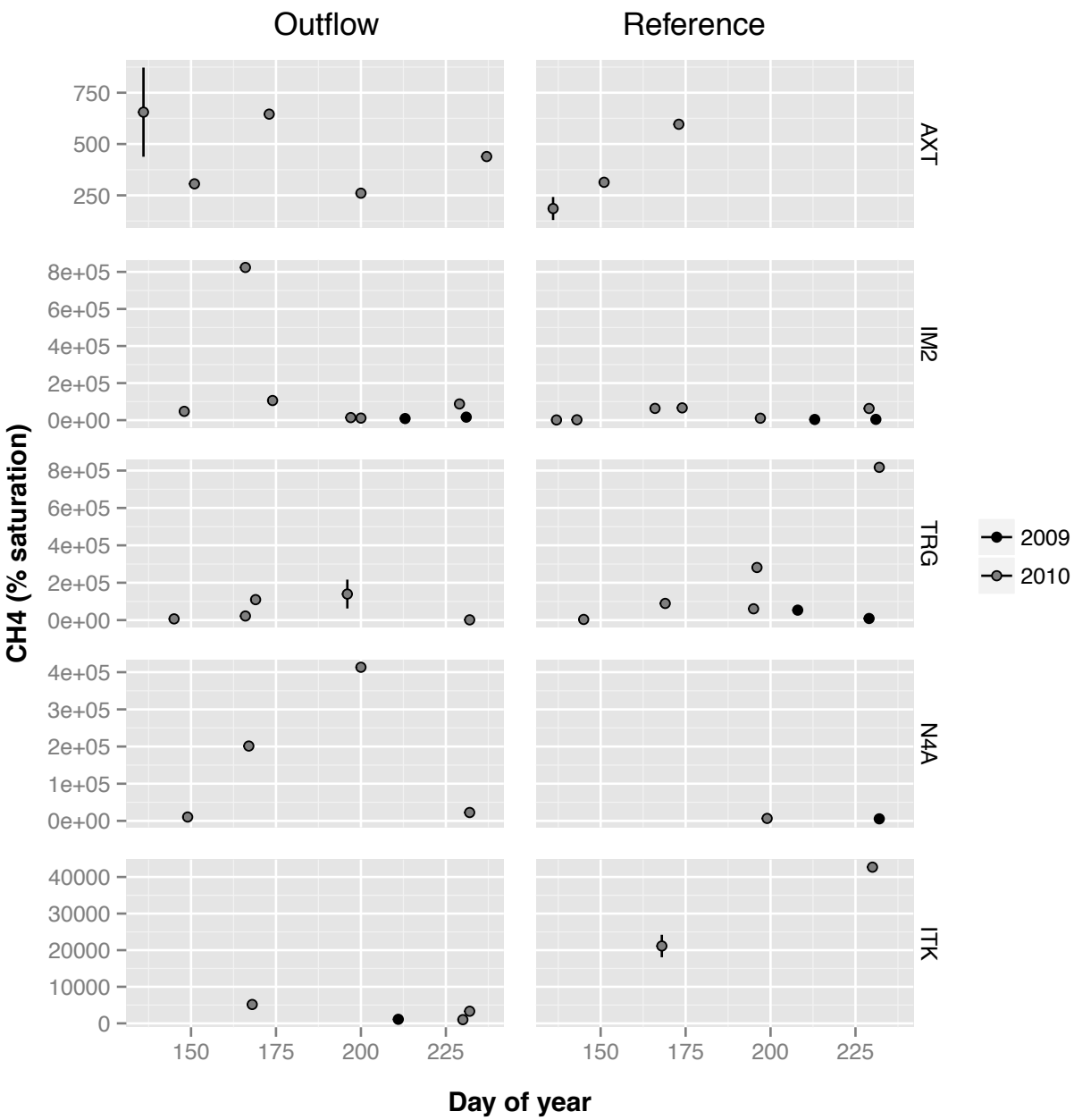

Figure S4. Dissolved CH_4 in % equilibrium concentration based on water temperature for the five sites near the Toolik Field Station where repeat measurements of feature outflow were made from 2009-2011. Symbology as in figure S1.

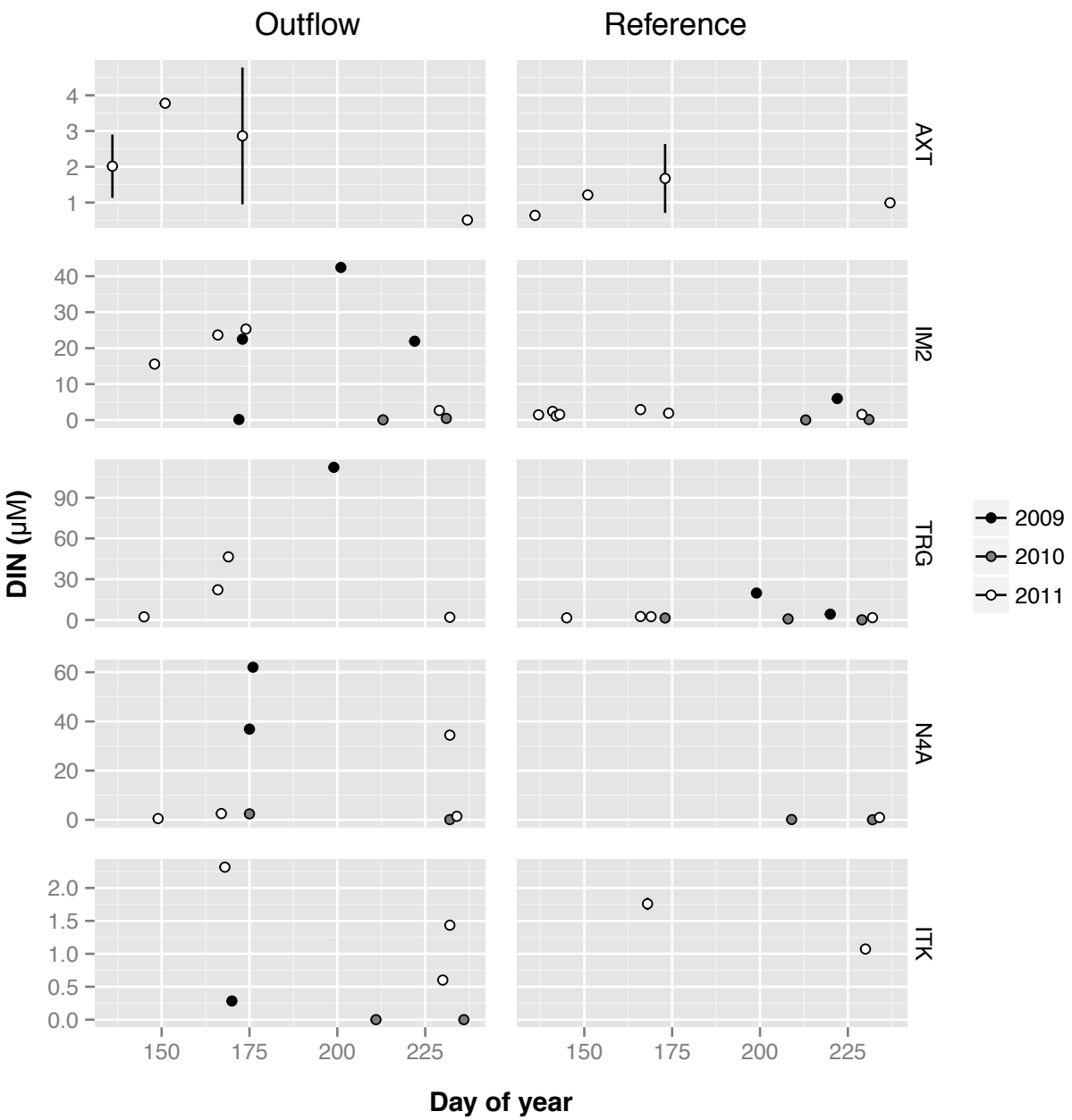

Figure S5. Dissolved inorganic nitrogen (DIN) concentration for the five sites near the Toolik Field Station where repeat measurements of feature outflow were made from 2009-2011. Symbology as in figure S1.

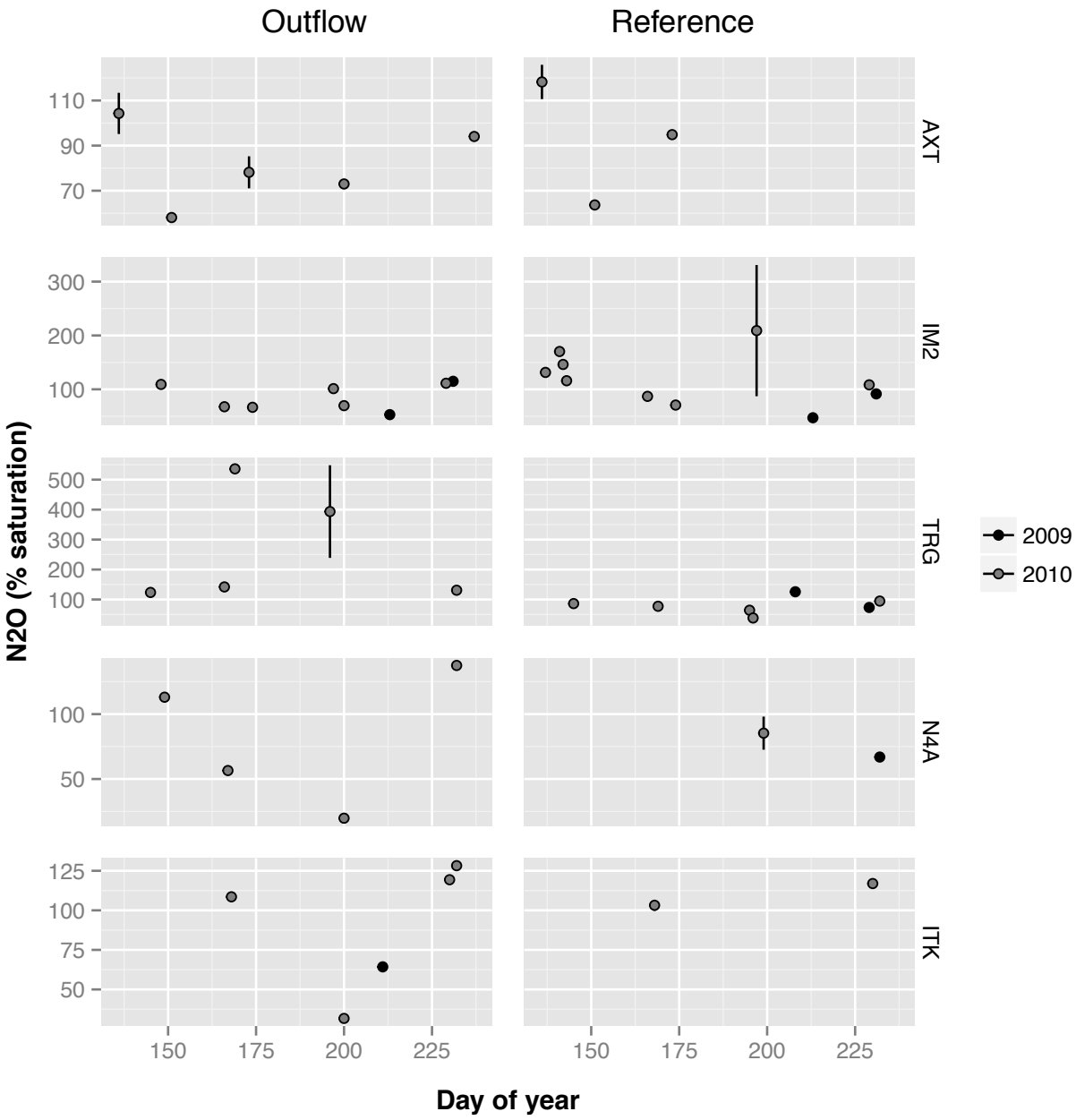

Figure S6. Dissolved N_2O in % equilibrium concentration based on water temperature for the five sites near the Toolik Field Station where repeat measurements of feature outflow were made from 2009-2011. Symbology as in figure S1.

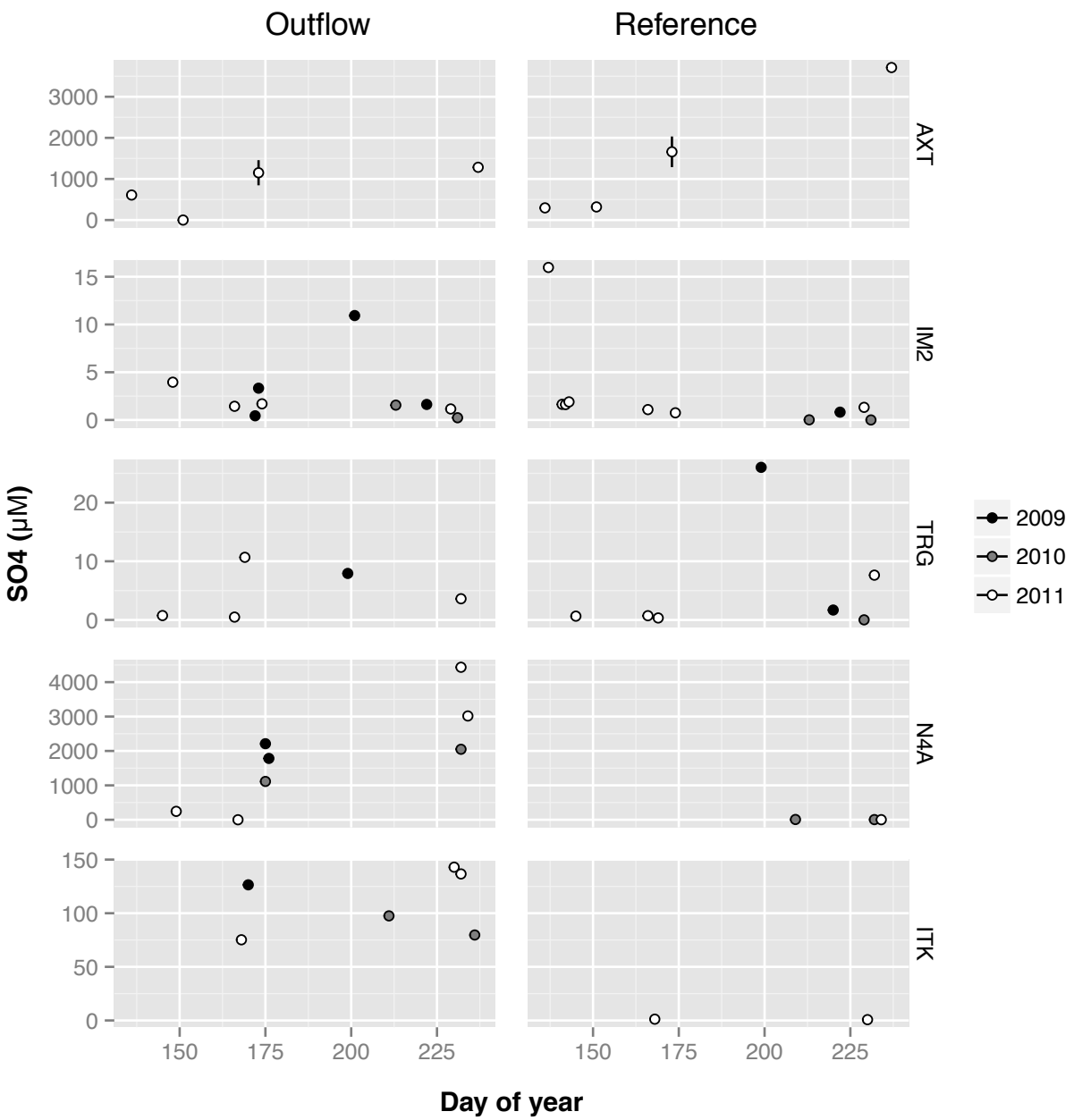

Figure S7. Dissolved sulfate concentration for the five sites near the Toolik Field Station where repeat measurements of feature outflow were made from 2009-2011. Symbology as in figure S1.

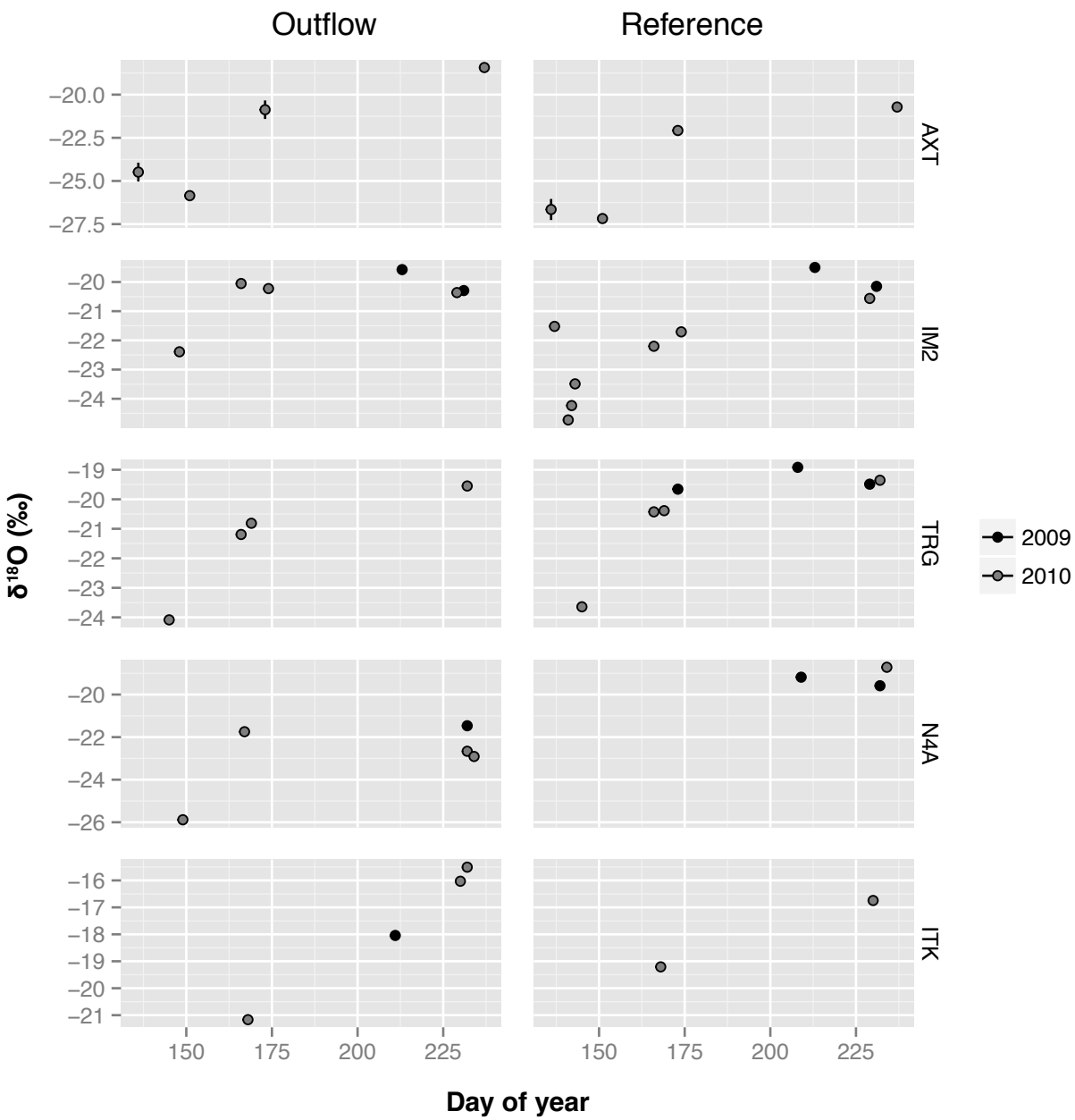

Figure S8. $\delta^{18}O$ signature for water draining the five sites near the Toolik Field Station where repeat measurements of feature outflow were made from 2009-2011. Symbology as in figure S1.